



LAWRENCE  
LIVERMORE  
NATIONAL  
LABORATORY

# Measurements of Ionic Structure in Shock Compressed Lithium Hydride from Ultra-fast X-ray Thomson Scattering

A. L. Kritcher, P. Neumayer, C. Brown, P. Davis, T. Doppner, R. W. Falcone, D. O. Gericke, G. Gregori, B. Holst, O. L. Landen, H. J. Lee, E. C. Morse, A. Pelka, R. Redmer, M. Roth, J. Vorberger, K. Wunsch, S. H. Glenzer

July 17, 2009

Physic Review Letter

## **Disclaimer**

---

This document was prepared as an account of work sponsored by an agency of the United States government. Neither the United States government nor Lawrence Livermore National Security, LLC, nor any of their employees makes any warranty, expressed or implied, or assumes any legal liability or responsibility for the accuracy, completeness, or usefulness of any information, apparatus, product, or process disclosed, or represents that its use would not infringe privately owned rights. Reference herein to any specific commercial product, process, or service by trade name, trademark, manufacturer, or otherwise does not necessarily constitute or imply its endorsement, recommendation, or favoring by the United States government or Lawrence Livermore National Security, LLC. The views and opinions of authors expressed herein do not necessarily state or reflect those of the United States government or Lawrence Livermore National Security, LLC, and shall not be used for advertising or product endorsement purposes.

# Measurements of Ionic Structure in Shock Compressed Lithium Hydride from Ultra-fast X-ray Thomson Scattering

A. L. Kritcher<sup>1,2</sup>, P. Neumayer<sup>1</sup>, C. R. D. Brown<sup>3,4</sup>, P. Davis<sup>1,5</sup>, T. Döppner<sup>1</sup>, R. W. Falcone<sup>5</sup>, D. O. Gericke<sup>6</sup>, G. Gregori<sup>7</sup>, B. Holst<sup>8</sup>, O. L. Landen<sup>1</sup>, H. J. Lee<sup>5</sup>, E. C. Morse<sup>2</sup>,

A. Pelka<sup>9</sup>, R. Redmer<sup>8</sup>, M. Roth<sup>9</sup>, J. Vorberger<sup>6</sup>, K. Wünsch<sup>6</sup>, and S. H. Glenzer<sup>1</sup>

<sup>1</sup>*L-399, Lawrence Livermore National Laboratory, P.O. Box 808, Livermore, CA 94551, USA*

<sup>2</sup>*Department of Nuclear Engineering, University of California Berkeley, Berkeley, CA 94709*

<sup>3</sup>*Department of Physics, Imperial College, London SW7 2AZ, UK*

<sup>4</sup>*AWE plc., Aldermaston, Reading, RG7 4PR, UK*

<sup>5</sup>*Department of Physics, University of California Berkeley, Berkeley, CA 94709*

<sup>6</sup>*Department of Physics, University of Warwick, Coventry CV4 7AL, UK*

<sup>7</sup>*Department of Physics, Oxford University, Oxford OX1 3PU, UK*

<sup>8</sup>*Universität Rostock, Institute für Physik, D-18051 Rostock, Germany*

<sup>9</sup>*Institut für Kernphysik, Technische Universität Darmstadt, Darmstadt, Germany and*

<sup>10</sup>*AWE plc., Aldermaston, Reading, RG7 4PR, UK*

(Dated: July 15, 2009)

We present the first ultrafast temporally, spectrally and angularly resolved x-ray scattering measurements from shock-compressed matter. These laser-compressed lithium-hydride samples are well characterized by inelastic Compton and Plasmon scattering of a K- $\alpha$  x-ray probe providing independent measurements of temperature and density. The experimental spectra yield the absolute elastic and inelastic scattering intensities from the measured density of free electrons. The data show excellent agreement with the total intensity and structure when using the two-species form factor and accounting for ionic screening.

PACS numbers: 52.25.Os, 52.35.Fp, 52.50.Jm

Keywords: K-alpha X-ray Scattering, Thomson Scattering, Compton Scattering, Shock Compression

Measurements of the compression and heating of shock-compressed matter are fundamental in the study and understanding of the physical and chemical properties of dense matter at high pressures. Dense matter conditions ( $> 1$  Mbar) occur in astrophysical objects, such as Jovian Planets [1, 2] and in inertial confinement fusion experiments [3, 4], predicted to compress material to pressures  $> 100$  Mbar. Investigation of the behavior of the ionic and electronic properties in this regime is important to determine the equation of state and thermodynamic properties of materials under extreme conditions.

With the use of powerful laser-produced x-ray scattering probes, information on the temperature, density, and ionization state of warm or hot dense matter has been studied [5–7]. In these first experiments from isochorically heated matter, Ly- $\alpha$  and He- $\alpha$  x-ray sources probed the collective and non-collective plasma regimes. More recently, experiments have characterized shocked-compressed matter [8–10] and measured the coalescence time of multiple shocks traveling through compressed material [10]. This characterization is important for inertial confinement fusion experiments that require a series of well-timed shocks to compress the fuel and ignite thermonuclear burn.

In this letter, we employ titanium K- $\alpha$  x-rays to characterize compressed matter and present the first ultrafast (10 ps) Thomson scattering measurements [11] as a function of wave-vector during shock compression. These laser driven experiments characterize the structure at

pressures of several Mbar and determine the thermodynamic properties of LiH targets. In contrast to previous studies [12, 13], present measurements of inelastic scattering spectra in the forward and backward scattering regimes provide accurate information on the temperature and density, and further yields the absolute ionic scattering component.

With the use of picosecond diagnostics, sub-ns dynamic material conditions can be probed, avoiding uncertainties due to temporal changes in the structure for shocked systems. We find that the data are sensitive to theoretical models that use the two-species dynamic scattering form factor [7, 14–16], and are in best agreement with models that further include screening effects to account for strong ion coupling i.e. a Screened One Component Plasma (SOCP) model [17] and calculations that use Density Functional Theory (DFT) [18].

Figure 1 at) shows a schematic of the experiment performed at the Titan laser facility, Lawrence Livermore National Laboratory [19]. In these experiments, 300  $\mu\text{m}$  thick solid density LiH foils ( $\rho_o=0.78\text{gcm}^{-3}$ ) have been compressed and heated by a factor of 2.7 times solid density using a 4 ns shaped laser beam ( $I_{\text{PEAK}}=2.5\times 10^{13}\text{Wcm}^{-2}$ , see Fig. 1 c)) that launched a strong shock into the material. An additional petawatt-class short pulse laser beam, delayed in time by  $t=4.5 \pm 0.3$  ns from the compression beam, was used to create ultrafast Ti K- $\alpha$  x-ray bursts with a temporal resolution of 10 ps [20] and bandwidth of  $\Delta E/E = 0.3\%$ ,

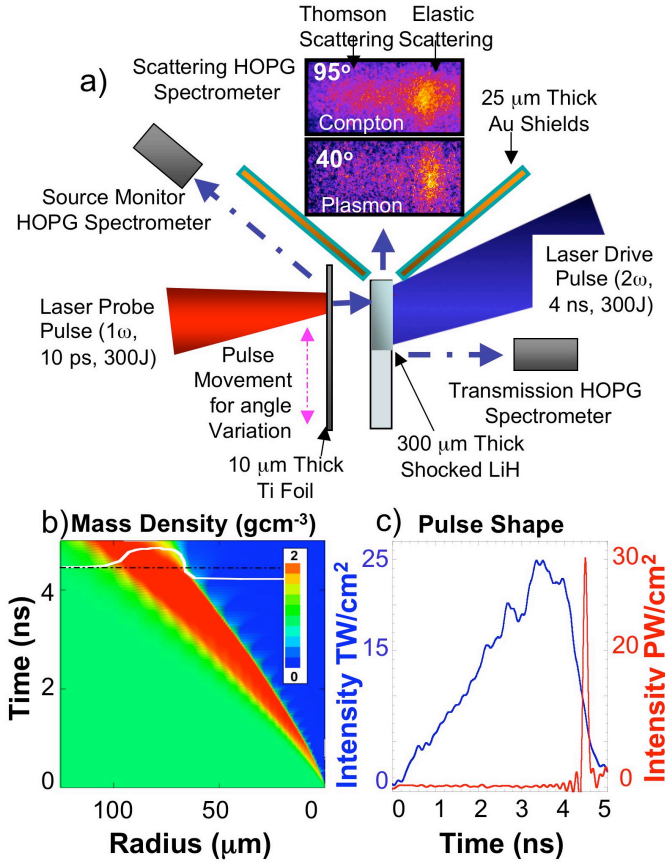


FIG. 1: a) Schematic of the experimental set-up. Here, short-pulse laser produced Ti K- $\alpha$  x rays are scattered from LiH targets that are compressed using a second long-pulse drive beam. Also shown are raw data for scattering at about  $95^\circ$  and  $40^\circ$ . b) Radiation-hydrodynamic calculations of the mass density, plotted as a function of time and target thickness, where  $t=0$  denotes the start of the drive beam. The predicted compression at  $t=4.5$  ns is about  $\rho/\rho_o = 2.7$ . c) Profiles of the measured drive-beam waveform (blue) and a delayed short-pulse beam that was used to create the x-ray probe (red).

that were scattered from the dense compressed plasma. Temporally, spectrally, and angularly resolved Thomson scattering measurements allows characterization of the plasma conditions from elastic and inelastic scattering in the non-collective and collective regimes, i.e. Compton and Plasmon features, which was recorded using a high reflectivity [21] curved graphite (HOPG) crystal, see Fig. 1 a). Shock wave heating of these solid density foils resulted in a Fermi-degenerate plasma, where the width of the Compton feature in the non-collective regime is a measure of the Fermi temperature, providing the electron density of  $1.6 \times 10^{23} \text{ cm}^{-3}$ . With the observation of inelastic scattering, the elastic feature can be absolutely calibrated, providing a measurement of the static ion-ion structure factor. The temperature, dependent on the total elastic scattering intensity, can then be inferred from

the scattering amplitude in the non-collective regime [17], yielding and electron temperature of  $T=1.7$  eV.

The K- $\alpha$  x-ray source was produced from  $3.6 \times 10^{16} \text{ Wcm}^{-2}$  short pulse laser irradiation of  $10 \mu\text{m}$  thick Ti foils. Approximately  $10^{12}$  photons on target enabled single shot accuracy, and the source probe energy (4.51 keV) was sufficient to penetrate through the dense plasma. Radiation-hydrodynamic simulations of the mass density, shown in Fig. 1b), were calculated from the measured heater beam waveforms using the 1D modeling code HELIOS [22]. Calculations predicted electron temperatures ranging from 1.3 to 1.8 eV. The calculated ionization state from radiation-hydrodynamic modeling was  $Z = 1$  for conditions at 2.6 to 2.9 times compression, resulting in densities ranging from  $1.5$ - $1.7 \times 10^{23} \text{ cm}^{-3}$ .

The scattering spectra were measured from the compressed LiH targets at angles ranging from about  $35$  to  $105$  degrees, corresponding to  $\alpha = 0.45$  to  $1.2$  where the collective ( $\alpha > 1$ ) and non-collective scattering ( $\alpha < 1$ ) regimes were accessed, probing the electron momentum distribution and electron plasma waves, respectively.

$$\alpha = \frac{1}{k\lambda_S} = \frac{\lambda}{2\pi\lambda_S} \quad (1)$$

Here,  $k$  is the magnitude of the scattering vector, where  $k = (4\pi E_0/hc) \sin(\theta_s/2)$ , and  $\lambda_S$  is the screening length. The parameters  $\theta_s$  and  $E_0$  are the scattering angle and energy of the incident x-ray probe, respectively. The scattering angle was varied by shifting the short pulse focus location on the Ti foil with respect to the scattering volume. Accuracy of the pointing resulted in an error of  $\pm 10^\circ$  due to the scattering geometry and range of  $k$ -vectors sampled by the finite exception angle of the spectrometer and the source size.

Figure 2 shows the Thomson scattering measurements in the non-collective regime for a scattering angle of  $95 \pm 10^\circ$  and at  $t = 4.5 \pm 0.3$  ns after the start of the heater beam. Theoretical fits to the experimental data [17] yield electron densities and temperatures of  $1.6 \times 10^{23} \text{ cm}^{-3}$  and 1.7 eV, with an error of about  $\pm 20\%$  due to noise in the experimental data. Here, we analyze data in the non-collective regime, i.e. large  $k$ , where additional error due to temperature dependence on theoretical models is small.

The parabolic Compton feature is downshifted in energy due to the Compton effect by  $\Delta E_c = \hbar^2 k^2 / 2m_e = 43 \text{ eV}$ . In the non-collective regime, the electrons are Fermi degenerate and the width of the down-scattered peak is proportional to the root of the Fermi temperature, i.e. reflecting the Fermi degenerate momentum distribution function. The densities inferred from the Compton feature are also consistent with the frequency shift of plasmon scattering at lower  $k$  values, providing a direct measure of the electron density. The temperature is inferred from the elastic scattering intensity, calibrated

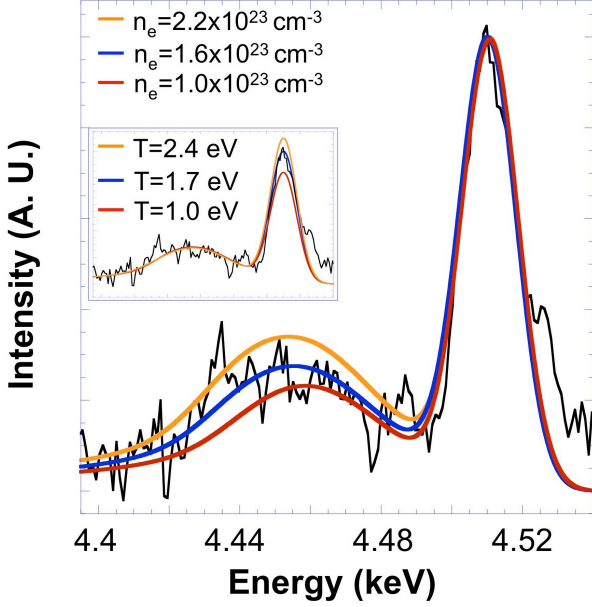


FIG. 2: X-ray Thomson scattering data from shock compressed LiH targets using Ti K- $\alpha$  x-rays in the non-collective scattering regime. The single-shot data at  $95 \pm 10^\circ$  show elastic scattering at 4.5 keV and inelastic Compton scattering at 4.45 keV, which allows characterization of the electron density and temperature. Theoretical fits to the experimental data are plotted for various densities and temperatures (inset). Best theoretical fits to the experimental data indicate temperatures and electron densities of  $1.7 \text{ eV} \pm 20\%$  and  $1.6 \times 10^{23} \text{ cm}^{-3} \pm 20\%$ .

from inelastic scatter, due to its dependency on the static ion-ion structure factor. The ionization state ( $Z = 1$ ), ionization of the 2s Li electron, is inferred from collective scattering measurements [10]. Scattering from the dense compressed region dominates the scattering signal, and the contribution to the scattered spectra from uncompressed material, mainly affecting the elastic feature, is subtracted from the spectra using measured scattering intensities from uncompressed targets. Also, with determination of the electron density from the width of the down-scattered feature, the free-free feature can be absolutely calibrated,  $S_{ee}(k, \omega) = 0.80$ , and the absolute elastic feature can be determined.

Figure 3 shows measurements of the frequency-integrated ion feature of the scattering spectrum, plotted as a function of wave vector. Here the scattered radiation power  $P_S(\mathbf{R}, \omega) d\Omega d\omega$  is dependent on the total dynamic structure factor of the electrons  $S_{ee}^{tot}(\mathbf{k}, \omega)$  according to

$$P_S(\mathbf{R}, \omega) d\Omega d\omega = \frac{P_0 r_0^2 d\Omega}{2\pi A} N S_{ee}^{tot}(\mathbf{k}, \omega) d\omega \quad (2)$$

$$\times |\hat{\mathbf{k}}_S \times (\hat{\mathbf{k}}_S \times \hat{\mathbf{E}}_O)|^2$$

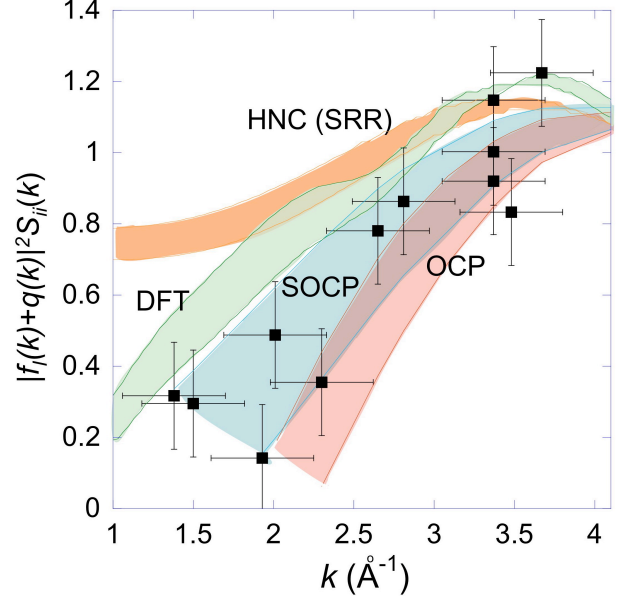


FIG. 3: Measurements of the elastic scattering intensity as a function of the scattering wave vector from shock compressed LiH targets using Ti K- $\alpha$  x-rays (black points). Also shown are theoretical models for the elastic scattering intensity, the red curve is the One Component Plasma (OCP) model that uses a Charged Hard Spheres (CHS) representation for the ions, and the blue curve is the Screened One Component Plasma (SOCP) model that applies a screening correction to the bare spheres in the OCP model. The orange curve uses hyper-netted chain equations (HNC) with SRR and the green curve are calculations using density functional theory (DFT) and molecular dynamics (MD).

The total dynamic structure factor,  $S_{ee}^{tot}(\mathbf{k}, \omega)$  describes the probability of finding a particle with respect to another particle in  $k$  space, and includes the elastic scattering feature which is strongly dependent on correlation effects for a strongly coupled plasma [15]

$$S_{ee}^{tot}(\mathbf{k}, \omega) = |f_I(k) + q(k)|^2 S_{ii}(\mathbf{k}, \omega) + Z S_{ee}^0(\mathbf{k}, \omega) + S_{bf}(k, \omega) \quad (3)$$

here,  $S_{ee}^0(\mathbf{k}, \omega)$  is the dynamic structure of the free electrons,  $Z$  is the ionization states, and  $S_{bf}(\mathbf{k}, \omega)$  is the bound-free feature. The first term is the ion scattering feature, which describes scattering from tightly bound electrons via the ion form factor,  $f_I(k)$ , and a screening cloud of valance electrons surrounding the ions via  $q(k)$ . Here,  $S_{ii}(\mathbf{k}, \omega)$  is the dynamic ion-ion structure factor. In this experiment, the ion-acoustic modes cannot be resolved, and the ion-ion structure factor is treated statically, i.e. frequency integrated, where  $S_{ii}(\mathbf{k}, \omega) \sim S_{ii}(\mathbf{k}) \delta(\omega)$  and  $\delta(\omega)$  is the Dirac delta function.

The absolute scattering intensities were compared between shots by measuring the number of source photons

produced in each shot and accounting for the source solid angle. Also taken into account is the dependency of the scattered power on polarization of the incident radiation for a given scattering angle. For unpolarized light from a laser-plasma source, this dependency is given by  $|\mathbf{k}_S \times (\mathbf{k}_S \times \mathbf{E}_0)|^2 = \frac{1}{2}(1 + \cos^2(\theta))$  in Eq. 2.

Also plotted in Fig. 3 are theoretical models for the elastic scattering intensity, dependent on static ion-ion structure factor values, that use the total two-species Chihara formula to calculate the total elastic scattering feature. The band of values for each model are calculated for a range of temperature and density conditions, that account for shot-to-shot variations in the drive beam waveform and intensity. Here, radiation-hydrodynamic modeling predicts changes in material conditions of  $< 1\%$  over the probe time, and a uniform compression region is probed by defocusing the drive beam to  $750 \mu\text{m}$  and using a phase plate to smooth the intensity profile.

The Screened One Component Plasma (SOCP) model [17] models the electrons as a neutralizing background and the ions are modeled as linearly screened, charged hard spheres, to account for short-range strong coupling effects. The hyper-netted chain equation model (HNC-Y) uses Yukawa potentials to account for screening effects and short range repulsion (SRR) was added to the Debye potential as an effective ion interaction potential [23]. Also plotted, are Density Functional Theory (DFT) calculations, coupled with molecular dynamics (MD) simulations [18].

These calculations use the two-species Chihara formula to calculate the ion feature [7], and are in good agreement with experimental data. Calculations that use single-ion species models overestimate the intensity of the scattered ionic feature by a factor of about 1.5 to 3. The total elastic scattering feature (Eq. 3) scales with the average of the square of the number of bound electrons  $Z_b^2 = \Sigma N^\alpha (Z_b^\alpha)^2 / \Sigma N^\alpha$ . Here,  $N^\alpha$  and  $Z_b^\alpha$  are the atomic number per molecule and number of bound electrons per species  $\alpha$ . Consequently, the ion feature for Li(+)H is smaller than for pure Li(+) at the same electron density. We further observe that the small k-vector-behavior is dependent on the approximation to the screening potential. Models that ignore screening effects, such as the One Component Plasma model (OCP), lie below the data for  $k < 3 \text{ \AA}^{-1}$ . Calculations using DFT-MD are in agreement with the data, but are slightly greater than measured values of the ion feature. The SOCP model offers better agreement with the measurements, indicating that the screened potentials best approximate the data. The SRR potential over-approximates the elastic scattering feature for small  $k$ .

In summary, we have measured the ionic structure of well characterized plasmas using spectrally resolved x-ray Thomson scattering in the collective and non-collective regime. A material compression of 2.7 times solid density was determined from inelastic Compton and plas-

mon scattering. We find that calculations for the ionic scattering component are sensitive to models that use two-species, and are in best agreement when screening is included. This result validates the use of elastic scattering to infer the ion temperature in dense plasmas. This result is also important for studying equation of state models for materials under extreme conditions, such as those encountered in laboratory astrophysics and in inertial confinement fusion experiments.

## ACKNOWLEDGMENTS

This work performed under the auspices of the U.S. Department of Energy by Lawrence Livermore National Laboratory under Contract No. DE-AC52-07NA27344. Work was also supported by the National Laboratory User Facility, Laboratory Directed Research and Development Grants No. 08-ERI-002 and No. 08-LW-004, by the Helmholtz association (VH-VI-104) and by the Deutsche Forschungsgemeinschaft (SFB 652). The work of G.G. was supported by EPSRC grant no. EP/G007187/1 and the Science and Technology Facilities Council of the United Kingdom.

- 
- [1] H. C. Connolly and Jr., Stanley G. Love, *Science* **280**, 62 (1998).
  - [2] T. Guillot, *Science* **286**, 72 (1999).
  - [3] E. I. Moses *et al.*, *Fusion Sci. Tech.* **47**, 314 (2005).
  - [4] J. D. Lindl *et al.*, *Phys. Plasmas* **11**, 339. (2004).
  - [5] S. H. Glenzer *et al.*, *Phys. Rev. Lett.* **98**, 065002 (2007).
  - [6] S. H. Glenzer *et al.*, *Phys. Rev. Lett.* **90**, 175002 (2003), *ibid* *Phys. Plasmas* **10**, 2433 (2003).
  - [7] G. Gregori *et al.*, *J. Quant. Spectrosc. Radiat. Transfer*, **99**, 225 (2006).
  - [8] H. J. Lee *et al.*, *Phys. Rev. Lett.* **102**, 115001 (2009).
  - [9] E. Garcia Saiz *et al.*, *Nature Physics* **4**, 940 (2008).
  - [10] A. L. Kritcher *et al.*, *Science*, **322**, 69 (2008), *ibid* *Phys. Plasmas* **16**, 056308 (2009).
  - [11] S. H. Glenzer and R. Redmer, *Rev. Mod. Phys.* (accepted Nov. 3, 2008).
  - [12] B. Barbrel, *et al.*, *Phys. Rev. Lett.* **102**, 165004 (2009).
  - [13] D. Riley, *et al.*, *Phys. Rev. Lett.* **84**, 8 (2000).
  - [14] J. Chihara, *J. Phys. F: Met. Phys.* **17**, 295 (1987).
  - [15] J. Chihara, *J. Phys. : Condens. Matter* **12**, 231 (2000).
  - [16] G. Gregori *et al.*, *Phys. Rev. E* **74**, 26402 (2006).
  - [17] G. Gregori *et al.*, *High Energy Den. Phys.* **3**, 99 (2007).
  - [18] K. Wünsch *et al.*, *Phys. Rev. E* **79**, 010201 (2009).
  - [19] P. Beiersdorfer *et al.*, NIFS Proceedings Series No. NIFS-PROC-57 (National Institute for Fusion Studies, Toki, Japan 2004), p. 40-46.
  - [20] S. Tzortzakis *et al.*, *J. Quan. Spectr. Trans.* **99**, 614 (2006).
  - [21] F. J. Marshall and J. A. Oertel, *Rev. Sci. Instrum.* **68**, 735 (1997).
  - [22] J. J. MacFarlane, *et al.*, *JQSRT* **99**, 381-397 (2006).
  - [23] K. Wünsch *et al.*, *Phys. Rev. E* **77**, 056404 (2008).